





RESEARCH PAPER

 OPEN ACCESS 

# The astrocyte-enriched gene *deathstar* plays a crucial role in the development, locomotion, and lifespan of *D. melanogaster*

Xiaoli Zhang<sup>a</sup>, Dongyu Sun<sup>a</sup>, Kyle Wong<sup>b</sup>, Ammar Salkini<sup>b</sup>, Hadi Najafi <sup>b,c</sup>, and Woo Jae Kim <sup>a,b</sup>

<sup>a</sup>The HIT Center for Life Sciences, Harbin Institute of Technology, Harbin, China; <sup>b</sup>Department of Cellular and Molecular Medicine, Faculty of Medicine, University of Ottawa, Ottawa, ON, Canada; <sup>c</sup>Department of Molecular, Cell and Cancer Biology, University of Massachusetts Chan Medical School, Worcester, MA, USA

## ABSTRACT

The *Drosophila melanogaster* brain is a complex organ with various cell types, orchestrating the development, physiology, and behaviors of the fly. While each cell type in *Drosophila* brain is known to express a unique gene set, their complete genetic profile is still unknown. Advances in the RNA sequencing techniques at single-cell resolution facilitate identifying novel cell type markers and/or re-examining the specificity of the available ones. In this study, exploiting a single-cell RNA sequencing data of *Drosophila* optic lobe, we categorized the cells based on their expression pattern for known markers, then the genes with enriched expression in astrocytes were identified. *CG11000* was identified as a gene with a comparable expression profile to the *Eaat1* gene, an astrocyte marker, in every individual cell inside the *Drosophila* optic lobe and midbrain, as well as in the entire *Drosophila* brain throughout its development. Consistent with our bioinformatics data, immunostaining of the brains dissected from transgenic adult flies showed co-expression of *CG11000* with *Eaat1* in a set of single cells corresponding to the astrocytes in the *Drosophila* brain. Physiologically, inhibiting *CG11000* through RNA interference disrupted the normal development of male *D. melanogaster*, while having no impact on females. Expression suppression of *CG11000* in adult flies led to decreased locomotion activity and also shortened lifespan specifically in astrocytes, indicating the gene's significance in astrocytes. We designated this gene as '*deathstar*' due to its crucial role in maintaining the star-like shape of glial cells, astrocytes, throughout their development into adult stage.

## ARTICLE HISTORY

Received 22 October 2023  
Revised 7 June 2024  
Accepted 11 June 2024

## KEYWORDS

single-cell RNA sequencing;  
astrocyte; male  
development; *deathstar*;  
*CG11000*; *Eaat1*; glia



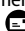

## Introduction

The *Drosophila melanogaster* nervous system is a powerful model to study development [1–4], physiology [4–6], and behaviors [7,8] of other organisms, including human, due to their great homology at cellular and molecular levels [9–12]. The *Drosophila* brain is composed of various cell types which are recognized primarily by their morphology and spatial organization [13–15], hence necessitating the study of this organ deeper at single-cell resolution.

In neuroscience, several classical cell type markers are commonly used to indicate and/or target a particular population of cells, considered to be the cells of a single type [16,17]. At least six main types of neural cells have been identified in

*D. melanogaster*, each characterized by the expression of a unique set of genes known as their molecular markers [16]. These cell types include perineurial glia (PNG), sub-perineurial glia (SPG), cortex glia (CG), astrocyte-like glia (ALG or astrocytes), ensheathing glia (EG) and neurons (Neu), each possesses its own genetic driver lines [16].

Since expression pattern of a single or multiple genes could not represent the full genetic profile of a particular cell [18,19], additional analyses are required for cell type identification. Also, besides the previously known molecular markers for each cell type, novel and/or uncharacterized genes may exist in *D. melanogaster* such that a specific cell type can be discerned with. With the advent of single-cell RNA sequencing (scRNA-seq), analysis

**CONTACT** Hadi Najafi  [hadi.najafihajivar@umassmed.edu](mailto:hadi.najafihajivar@umassmed.edu) Department of Molecular, Cell and Cancer Biology, University of Massachusetts Chan Medical School, Worcester, MA 01605, USA; Woo Jae Kim  [wkim@hit.edu.cn](mailto:wkim@hit.edu.cn)  The HIT Center for Life Sciences, Harbin Institute of Technology, Harbin 150001, China  
 Supplemental data for this article can be accessed online at <https://doi.org/10.1080/19336934.2024.2368336>

© 2024 The Author(s). Published by Informa UK Limited, trading as Taylor & Francis Group.

This is an Open Access article distributed under the terms of the Creative Commons Attribution License (<http://creativecommons.org/licenses/by/4.0/>), which permits unrestricted use, distribution, and reproduction in any medium, provided the original work is properly cited. The terms on which this article has been published allow the posting of the Accepted Manuscript in a repository by the author(s) or with their consent.

of the entire transcriptome of an individual cell is feasible, which facilitates determination of the identity of the cells in all organisms including *D. melanogaster*. By providing the full genetic profile of individual cells, scRNA-seq is a convenient strategy to identify novel cell types [20–22] and to re-examine the specificity of the pre-existing molecular markers in the respective cell types [23,24].

In this study, we take the advantages of the availability of the scRNA-seq data of *Drosophila* brain to perform clustering of the sequenced single cells of *Drosophila* brain based on their known molecular markers as well as their entire transcriptome, then seeking for novel genes with differential expression pattern across the clusters. Thereafter, the predicted expression pattern and functional role of the candidate genes are assessed experimentally.

## Materials and methods

### Datasets

A single-cell RNA-sequencing (scRNA-seq) data belonging to the *Drosophila* optic lobe was obtained from the NCBI Gene Expression Omnibus (GEO) database (accession number: GSE103771), which covered the expression profile of 17,272 *Drosophila* genes in a population of 120,000 single cells from optic lobe [25].

Another single-cell RNA-sequencing (scRNA-seq) data was from the *Drosophila* mid-brain and was obtained from the NCBI Sequence Read Archive (SRA) database (accession number: SRP128516), which covered the expression profile of 12,868 *Drosophila* genes in a population of 28,695 single cells from mid-brain [26].

Two bulk RNA-sequencing data of *Drosophila* whole brain were obtained from the NCBI GEO: one contained the expression profile of all *D. melanogaster* genes across four different developmental stages (days 5, 20, 30, and 40 posteclosion; accession number: GSE107049) [27] and another one contained the expression profile of all *D. melanogaster* genes across three different developmental stages of the fly (days 3, 7, and 14 posteclosion; accession number: GSE199164).

### Bioinformatics analyses

In order to have a set of clusters comprising the main neural cell types of *D. melanogaster* (i.e. PNG, SPG, CG, EG, ALG, and neurons), first, the expression matrix belonging to the scRNA-seq data of *Drosophila* optic lobe in the study of Konstantinides et al. (accession number: GSE103771) [25] was downloaded and used for downstream analyses. Then, this matrix was analyzed in accordance with the expression pattern of the previously known *Drosophila* marker genes specific to PNG, SPG, CG, EGN, EGT, ALG, and neuronal cell types and the single cells expressing the markers of a respective cell type and negative for the expression of the markers of other cell types were identified and presented as a heatmap of expression level using the online tool Heatmapper [28] with color codes (red and black colors refer to positive and negative expression for the markers, respectively).

To confirm the above-mentioned cell type classification, hierarchical clustering was performed in accordance with the similarities between the identified single cells based on their transcriptome profile and expressed as a heatmap with color codes for the Pearson correlation coefficient, using the ggplot2 [29] and pheatmap [30] packages in R. Also, principal component analysis (PCA) was performed to distinguish the cells/clusters with distinct transcriptome profile, using R program.

The lists of differentially expressed genes (DEGs) between clusters of interest were identified by the R package limma [31], considering the  $\log_2$  fold-change ( $\log_2FC$ )  $\geq 1$  and  $P$ -value  $< 0.05$  as the significance cutoff.

To confirm the differential expression pattern of the candidate genes in a particular cell type/cluster, the unpaired t-test method [32] was applied considering adjusted  $P$ -values (Benjamini–Hochberg correction)  $< 0.01$  and  $\log_2FC \geq 1$  as the significance cutoff. Venn diagram was performed for obtaining the list of common DEGs between the examined clusters, using the web-based tool Venny [33]. Pairwise alignment between the transcripts of CR34335 and CR40469 genes was performed in ClustalW [34,35].

### Fly stocks and crosses

All the *D. melanogaster* lines in this study were obtained from the Bloomington *Drosophila* Stock

Center (BDSC) and Vienna Drosophila Resource Center (VDRC). After being subjected to stocks, they were cultured in standard conditions (standard cornmeal-agar yeast fly food at 25°C in a 12 h light:12 h dark condition) following the previous description [36]. CO<sub>2</sub> served as an anesthetic.

For the crosses of fluorescence labeling experiments, the two binary systems GAL4/UAS-mCD8RFP and LexA/LexAop-mCD8GFP were employed simultaneously in individual male and female flies. The ALG cells of *Drosophila* CNS were labeled in accordance with the expression of a membrane-bound GFP (mCD8GFP) under the control of *Eaat1* gene promoter, fused to the sequence of LexA (*Eaat1-LexA*) (BDSC#: 52719).

Transgenic fly lines carrying the *CG11000* (*deathstar*)-*GAL4* were used to drive the expression of a membrane-bound RFP (mCD8RFP) in progenies (both in female and male) under the control of *deathstar* gene promoter (BDSC#: 72713, 23416, 91441). Therefore, the expression pattern of RFP will reflect the pattern of *deathstar* promoter activity across the *Drosophila* single cells. Table 1 lists the fly stocks and the crossing scheme for immunostaining experiments.

For functional analysis of the genes, the GAL4/UAS-RNAi system [37] was employed to deplete the function of genes of interest in a cell type-specific manner. Table 2 summarizes the fly stocks (parents) together with their crossing

**Table 1.** Crossing scheme for imaging experiments of the *Drosophila* brain. The line a contains RFP and GFP reporter genes under the control of UAS and LexAop sequences, respectively. Line B expresses LexA protein in an ALG-specific manner driven by *Eaat1* promoter. The fly line C (of F<sub>1</sub> generation) was generated by crossing the lines a and B (parents), and then it was crossed to the *CG11000-GAL4* line (i.e. D) to produce F<sub>2</sub> generation. Among the flies of F<sub>2</sub> generation, the males and females that lacked balancer chromosomes but contain the complete components of the two binary systems UAS/GAL4 and LexA/LexAop were selected for brain dissection. The females (♀) of all crosses were virgin.

Lines	Fly stocks (genotype & BDSC ID)	Cross scheme
A	<i>UAS-mCD8RFP, lexAop-mCD8GFP; Sp/CyO; TM2/TM6B</i> (# 32229)	P: A ♀ X B ♂
B	<i>w<sup>-</sup>; Eaat1-LexA/CyO; TM2/TM6B</i> (#52719)	↓
C	<i>UAS-mCD8RFP, lexAop-mCD8GFP; Eaat1-LexA/CyO; TM2/TM6B</i> (This study)	F1: C ♀ X D ♂
D	<i>w<sup>-</sup>; +/+; CG11000-GAL4</i> (BDSC #72713, 23416, 91441)	↓
		F2: E ♂ or ♀
E	<i>UAS-mCD8RFP, lexAop-mCD8GFP; Eaat1-LexA/+; TM6B/CG11000-GAL4</i> (This study)	↓
		CNS dissection

**Table 2.** Summary of the crosses and experimental genotypes for behavioral analyses. To generate the transgenic flies with expression of *CG11000-RNAi* in cell type-specific manner, the male flies of different GAL4 driver lines were crossed to the females harboring *UAS-CG11000-RNAi* in their genome (BDSC#: 51918). All the females (♀) for the above-mentioned crosses were virgin. Among the progenies of the above-described crosses, the flies with proper genotypes (harboring both cell type-specific expression of GAL4 and *UAS-CG11000-RNAi*) were selected based on the absence of balancer chromosomes (e.g. *CyO*, *TM3*, and *TM6B*). Three RNAi lines (BDSC# 51918, VDRC# v107504 and VDRC# v102061) have been used to confirm the functional role of *deathstar* gene in astrocytes.

Parents of the crosses (genotype & BDSC or VDRC ID)		Progeny phenotypes (♀ and ♂)	RNAi-expressing cell type
UAS-RNAi transgenic line (♀)	GAL4 driver lines (♂)		
<i>w<sup>-</sup>; +/+; UAS-C11000-RNAi</i> (# 51918)	<i>w<sup>1118</sup>; +/+; +/+</i>	wild type	-
<i>w<sup>1118</sup>; +/+; +/+</i>	<i>w<sup>1118</sup>; +/+; btn-GAL4/TM6B</i> (#45914)	wild type	-
<i>w<sup>-</sup>; +/+; UAS-C11000-RNAi</i> (# 51918)	<i>w<sup>1118</sup>; +/+; shn-GAL4/TM3</i> (#40436)	Non-TM3	PNG
	<i>w<sup>1118</sup>; +/+; Mdr65-GAL4/TM3</i> (#50472)	Non-TM3	SPG
	<i>w<sup>1118</sup>; +/+; CG-GAL4/TM3</i> (#45784)	Non-TM3	CG
	<i>w<sup>1118</sup>; +/+; CG9657-GAL4/TM3</i> (#39157)	Non-TM3	EGN
	<i>w<sup>1118</sup>; +/+; Drgx-GAL4/TM3</i> (#39908)	Non-TM3	EGT
	<i>w<sup>1118</sup>; +/+; nSyb-GAL4/TM6B</i> (#68222)	Non-TM6B	Neurons
<i>w<sup>-</sup>; +/+; UAS-C11000-RNAi</i> (BDSC# 51918, VDRC# v107504, v102061)	<i>w<sup>1118</sup>; +/+; btn-GAL4/TM6B</i> (#45914)	Non-TM6B	ALG

schemes, ensuring progenies to express the *deathstar* RNAi in a cell type-specific manner. In detail, the virgin females transgenic for the *UAS-deathstar RNAi* constructs (BDSC#: 51918, VDRC#: v107504, v102061) were crossed to different male driver lines expressing GAL4 under the control of the promoter of a set of cell type-specific genes (Table 2). The promoter of *shn* gene drives GAL4 expression in PNG, *Mdr65* in SPG, *wrapper* in CG, *CG9657* in EGN, *CG34340* (*Drax*) in EGT, *CG5264* in ALG, *repo* in all glia, and *nSyb* drives GAL4 expression in neurons [16,23,38]. After crossing the flies, the progenies with complete components of the GAL4/UAS binary system (i.e. *x-GAL4 > UAS-deathstar RNAi*) were collected based on their phenotypes (Table 2) and functional analyses of *deathstar* gene were performed for them.

As the control group of the experiment, flies without expression of *deathstar* RNAi but with the same genetic background were used. In fact, the flies of the control group contained the *UAS-deathstar RNAi* construct in their genome but lacked any expression of GAL4 proteins. Thus, no functional RNAi will be produced in this group.

### Immunostaining and imaging

Immunostaining was performed according to the previously-reported protocols [39,40]. In brief, brains were dissected from adults 5 days after eclosion, fixed with 4% formaldehyde for 30 min at room temperature, washed with 1X PBST (1X PBS containing 0.5% Triton-X100) three times (30 min each) and blocked in 5% normal donkey serum for 30 min. The brains were then incubated with primary antibodies in 1X PBST at 4°C overnight, followed by incubation with fluorophore-conjugated secondary antibodies for 1 hour at room temperature. Subsequently, brains were mounted with anti-fade mounting solution (Invitrogen, catalog number S2828) on slides for imaging.

The primary antibodies were chicken polyclonal anti-GFP (Aves Labs, catalogue number GFP-1010, 1:1000 diluted), rabbit polyclonal anti-RFP (Invitrogen, catalog number 710,530, 1:250 diluted) and mouse monoclonal anti-Bruchpilot (nc82) (DSHB, ID AB-2314866, 1:50 diluted). The applied fluorophore-conjugated secondary

antibodies comprised Alexa Fluor 488-conjugated goat anti-chicken (Invitrogen, catalog number A32931, 1:100 diluted), RRX-conjugated donkey anti-rabbit (Jackson Laboratory, catalog number AB-2340613, 1:100 diluted), and Dylight 405-conjugated donkey anti-mouse (Jackson Laboratory, catalogue number AB-2340839, 1:100 diluted). Fluorescence imaging with maximum projections of z-stacks was performed under a confocal laser scanning microscope (Zeiss LSM 7 MP) and the acquired images were processed using the NIH ImageJ [41], and presented by Adobe Illustrator CC 2023 for Mac.

### Colocalization analysis

To perform colocalization analysis of multicolor fluorescence microscopy images, the ImageJ software was used. Initially, the individual channels of the fluorescence image were merged to create a composite view. Then, in the 'Image' menu, we selected 'Type', and then selected 'RGB Color' to ensure the images are displayed in the correct color format. Next, we navigated to 'Image', then 'Adjust' and selected 'Color Threshold', and adjusted the threshold settings to isolate the yellowish pixels indicative of colocalization, and confirmed the selection by clicking the 'Select' button. Subsequently, we proceeded to 'Analyze', and 'Measure' buttons. This action will open a new window displaying the measurement data for the selected area. The 'Area' value provided in the measurement window was recorded, as it corresponds to the area of colocalization between the two fluorophores. To calculate the percentage of the colocalized area relative to the total area of the fluorophore of interest (e.g. GFP or RFP), we readjusted the threshold settings to encompass the entire fluorophore area, then clicked on 'Select' again. Afterward, we repeated the measurement process by going to 'Analyze' and then 'Measure' options. This will yield the total area value for the respective fluorophore. Finally, to determine the colocalization percentage, the area values of the colocalized regions were divided by the total area values of total GFP or RFP regions. This calculation provides the colocalization level within the specified region. A representative image of three independent fluorescence imaging experiments

with their colocalization regions were then presented. Also, the images were processed with ImageJ software using a threshold function to differentiate fluorescence from background. All specimens were imaged under identical conditions.

### **Developmental assay**

To assess the possible function of *deathstar* gene in the development of *D. melanogaster* from pupae to adulthood stage, the newly eclosed *D. melanogaster* of the crosses in Table 2 was collected and counted based on their genotypes. After counting, data were presented as the percentage of male and female flies expressing *deathstar* RNAi to the total number of eclosed flies.

### **Locomotion assay**

We recorded locomotion behaviors of the flies expressing *deathstar* RNAi in astrocytes, and their behaviors were compared to the control group. For this purpose, three different *deathstar* RNAi lines were tested, and the flies without expression of *deathstar* RNAi but with the same genetic background were used as control groups (Table 2). To restrict the expression of RNAi in adult flies, we raised them at 18°C before they eclosed and then transferred them to 29°C following eclosion for locomotion tests. To image fly locomotion, a custom LED array was placed under the stage to serve as backlight. A 2-mm transparent acrylic board sheet was placed on top of the LED array to produce homogeneous illumination. Fly behaviors were recorded using a camera with 1920 × 1080 30 Hz (1080p30). Behavioral arenas were custom built from opaque transparent acrylic board sheets. Chambers were 30 mm in diameter and 2 mm in height. Each fly group was aspirated into a separate chamber and placed on the stage. Flies were observed for 30 min to ensure that no gross motor defects were present before video acquisition was initiated.

### **Video acquisition and tracking**

Videos were acquired using camera at 1920 × 1080 30 Hz (1080p30). Image segmentation was performed by the custom software Fly Trajectory Dynamics Tracking (FlyTrDT) in python; First,

FlyTrDT identifies and quantifies fruit flies into elliptical pixels, and we extracted 2 main features from the videos: 1) The average forward speed and 2) The trajectory map of the fly group in each chamber. For the average forward speed of each group, FlyTrDT records the moving speed of each indoor fruit fly and analyzes the average speed of 10 fruit flies per second. For the trajectory map, FlyTrDT records the movement of each indoor fruit fly, then analyzes and plots the movement trajectories of 10 fruit flies in each chamber, including the movement trajectories of the entire group and the movement trajectories of each fruit fly in the group [42,43].

### **Lifespan assay**

Lifespan was measured at room temperature according to the standard protocols [44]. In brief, newly eclosed flies (0 to 3 days) were collected (50 per genotype) and then placed in two vials (25 flies per vial), and transferred to fresh vials every two days. Survival was recorded for each genotype (sum of two vials). We scored flies stacked in the food as death events in all the vials analyzed. The survival curves was created with Prism version 10 (GraphPad Software, San Diego, CA, USA) using the method of Kaplan and Meier [45]. For statistical significance of the experiment, one-way ANOVA method was used, and the death rate of each genotype was compared to control group which contained the flies without expression of *deathstar* RNAi but with the same genetic background. *P*-values <0.01 indicated the differences that achieved statistical significance.

### **Statistical analysis**

Statistical analysis and graphic representations were conducted using Prism 10 for Mac (GraphPad Software, San Diego, CA, USA). Unpaired t-test or one-way ANOVA (using the Bonferroni's multiple comparison) were applied, which was dependent on the measurements analyzed in the corresponding experiment. The averages with ± SEM in all cases were plotted. *P*-values were determined through two-tailed unpaired Student's t-test, unless otherwise specified, using GraphPad Prism 10 software. \**P* < 0.05; \*\**P* < 0.01; \*\*\**P* < 0.001, and \*\*\*\**P* < 0.0001.

## Results

### Cell-type identification of single cells in the *Drosophila* optic lobe

Each cell type of *Drosophila* central nervous system is characterized by expression of a unique set of genes, known as their molecular markers [15,16,46]. We used these markers (Figure 1a) to identify the type of single cells in the *Drosophila* optic lobe, sequenced by Konstantinides et al. [25], so that a particular cell type is positive for expression of its markers while negative for expression of the markers of other cell types. Based on these criteria, 156 single cells were identified as neurons, being positive for *nSyb* [47,48] and *elav* expression [49] while negative for all glial markers; 80 single cells were identified as ALG, positive for expression of five astrocytic markers (*Eaat1* [10,50], *almr* [51,52], *Gs2* [51,53], *ebony* [50,54] and *Gat* [10,55]) and lacking the expression of the markers of other glia and neurons. Also, expression pattern analysis of the markers specific to PNG: *CG4797* [25,56], *shn* [16] and *gem* [25], SPG: *Mdr65* [9] and *moody* [57,58]), CG: *Cyp4g15* [59,60] and *wrapper* [25,56] and EG: *CG9657* [50,61,62] and *CG34340* [16,62], has identified 56 single cells, we assigned them all as non-ALG glia or other glia (Figure 1b).

Analysis of the global transcriptome profile of the identified cells through principal component analysis (PCA) illustrated a clear separation of ALG single cells from single cells of other cell types (Figure 1c). Further classification of the identified single cells was performed via hierarchical clustering based on the correlation coefficient of their transcriptome profile, and results illustrated four different clusters for ALG cells (clusters 1–4), three clusters for neuronal cells, and two additional clusters which were mixes of neurons and non-ALG glia (Figure 1d).

To identify the ALG-enriched genes, differential gene expression analysis was performed between each ALG cluster and all clusters of other cell types. Results showed that among all sets of differentially expressed genes (DEGs), the differential expression pattern of 17 genes was common between all ALG clusters, of which eleven genes showed enrichment (Figure 1e), while six genes showed depletion (Figure 1f) in ALG. In

fact, the ALG clusters 1 to 4 all showed the enriched expression of some previously known glial markers such as *CR34335* [63], *Inx2* [64–66], and *Nrv2* [23,26,67] and also enriched expression of the astrocyte markers *CG9394* [51], *Eaat1* [25,50,68], *Gat* [50], *Gs2* [25,69], and *CG1552* [51] (Figure 1e; table), while they exhibited the depleted expression of the markers of other cell types (e.g. *gem* and *CG4797* (the PNG markers), *moody* (a SPG marker), *wrapper* (a CG marker), and *CG34340* (a EG marker)) (Figure 1f; table), supporting the identity of the clusters 1 to 4 as astrocytes. The full list of DEGs is presented in Supplemental file S1.

Among the identified ALG-enriched genes (Figure 1e; table), *CR40469* and *Eaat1* were previously classified by Konstantinides et al. in neuronal clusters (clusters # 23, 43, and 45 in their study) [25], while *Eaat1* is a well-characterized marker for astrocytes [6,10,51,68,70,71], and no cell type-specificity was reported yet for *CR40469* gene.

Sequence analysis of *CR40469* transcript (GenBank No: NR\_003723.2) demonstrated that it has 96.73% identity with the transcript of the glial marker *CR34335* (GenBank No: NR\_133508.1) (Figure 1g), raising the hypothesis that the expression level reported for the *CR40469* in *Drosophila* optic lobe single cells could be influenced by this high-degree sequence homology, hence both transcripts similarly map against *Drosophila* genome leading to highly similar expression counts for both genes. Expression correlation analysis of these genes across all sequenced single cells of *Drosophila* optic lobe ( $n = 120,000$  cells) showed a remarkable positive correlation between their expression level ( $R^2 = 0.93$ ,  $P < 0.0001$ ), strengthening this hypothesis (Figure 1h).

*Eaat1* is a known glial marker which is predominantly expressed in astrocytes [72]. To study which gene(s) is/are co-expressed with it, first the sequenced single cells of the *Drosophila* optic lobe [25] were categorized based on their expression pattern for *Eaat1*, then differential gene expression analysis was performed between the cells 'with' and 'without' *Eaat1* expression (assigned them as *Eaat1*<sup>+</sup> and *Eaat1*<sup>-</sup> cells, respectively). Results highlighted the differential expression of an uncharacterized gene *CG11000* whose expression was significantly

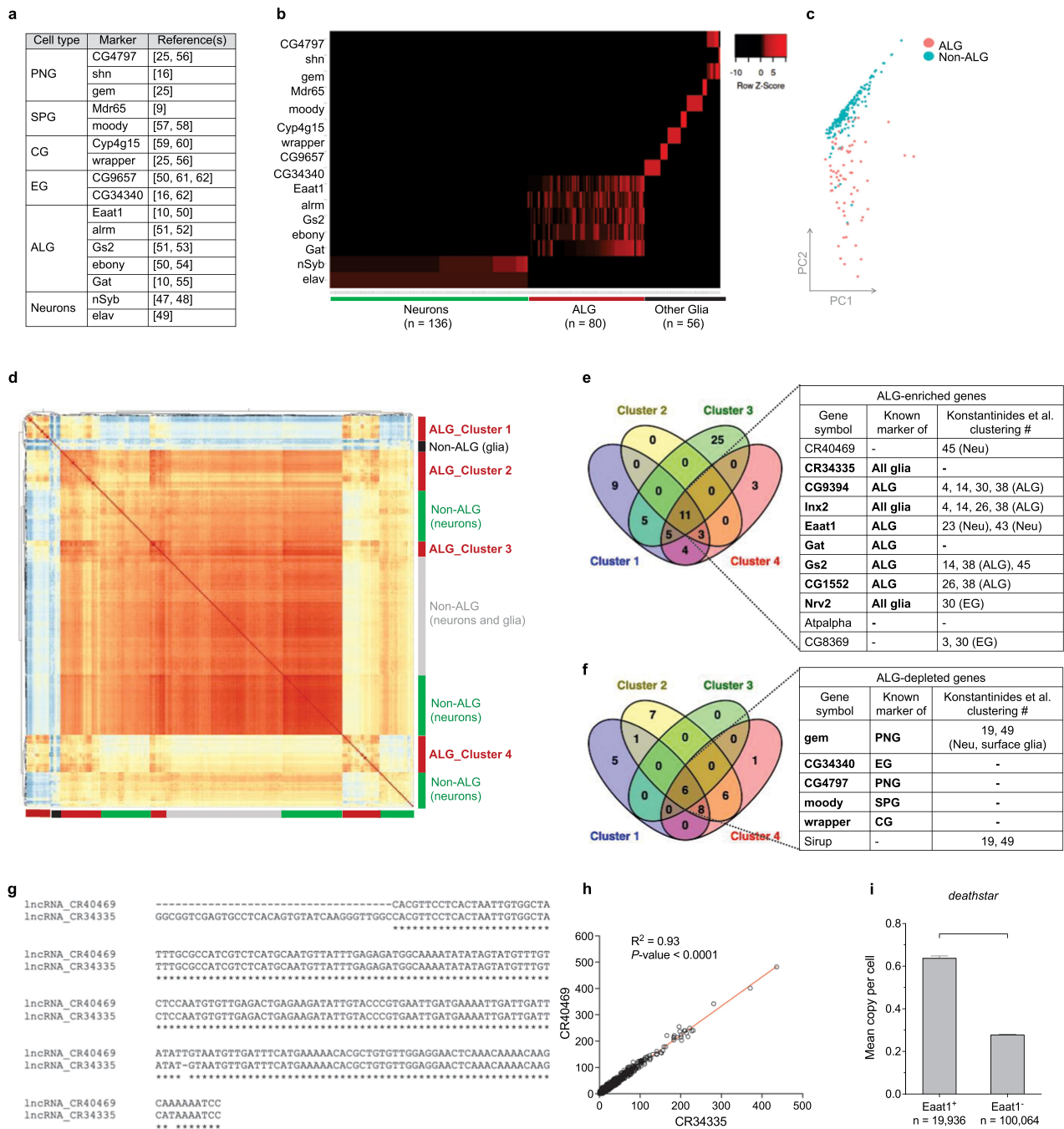


**Figure 1.** Cell type identification of single cells in *Drosophila* optic lobe. (a) the list of molecular markers used in this study for cell type identification. (b) Classified single cells of *D. melanogaster* optic lobe based on their expression pattern for the markers. Red color denotes 'expression,' and black color denotes 'no expression.' A row Z-score was used to represent the expression level of each marker. (c) The principal component analysis (PCA) plot distinguishing the ALG single cells (red dots) from single cells of other cell types (labeled as non-ALG, green dots) based on their entire transcriptome profile. (d) Hierarchical clustering categorized ALG cells into four different clusters, all exhibiting distinct global transcriptome profile from other cell types. (e) Venn diagram illustrates the number of the genes upregulated in each ALG cluster. The table lists the common upregulated genes between all ALG clusters. Bold-face fonts represent the genes with cell type-specificity reports in previous studies. If the genes were previously attributed to a particular cell type cluster by Konstantinides et al. [25], the features of the clusters are presented in the table. (f) Venn diagram illustrates the number of downregulated genes in each ALG cluster. The table lists the common downregulated genes in all ALG clusters. Also, the clustering information of Konstantinides et al. study is presented for each gene. (g) Sequence homology between *CR40469* and *CR34335* transcripts using ClustalW. Both sequences are shown in 5' → 3' orientation. (h) Positive expression correlation of *CR40469* and *CR34335* genes in *Drosophila* optic lobe ( $n = 120,000$  single cells). (i) Increased expression of *deathstar* gene in *Eaat1*<sup>+</sup> cells in *Drosophila* optic lobe.

higher in *Eaat1*<sup>+</sup> cells (2.43 folds increase, *P*-value <0.0001) (Figure 1i), suggesting potential astrocytic function of this gene (similar to *Eaat1* gene). The full list of the upregulated genes in *Eaat1*<sup>+</sup> cells is presented in the supplemental file S2.

### Positive expression correlation of *deathstar* with *Eaat1* in *Drosophila* brain

The gene *CG11000* was named ‘*deathstar*’ due to its crucial role in determining the fate of star-shaped astrocytes in fruit flies, referencing the iconic space station from Star Wars. The *deathstar* gene is implicated in the regulation of cell differentiation, predicted to be located in the membrane, and expressed in the adult head [73]. Given the increased expression level of *deathstar* gene in *Eaat1*<sup>+</sup> cells, its expression pattern was compared to the expression pattern of the previously known cell type markers of *D. melanogaster* across full set of single cells in the *Drosophila* optic lobe. Results showed a positive expression correlation between *deathstar* and *Eaat1* genes, as well as the coclustering pattern of these genes in the resultant heatmap (*n* = 120,000 cells) (Figure 2a). The positive expression correlation of *deathstar* and *Eaat1* genes was also observed in the single cells of *Drosophila* mid-brain (*n* = 28,695 cells), sequenced by Croset et al. [26] (Figure 2b).

Moreover, the expression level of *deathstar* and *Eaat1* genes was examined in a bulk RNA-seq data of developing *Drosophila* whole brain (GSE107049) [27] and results consistently demonstrated a significant positive correlation between the expression level of these genes in females ( $R^2 = 0.7579$ , *P*-value = 0.0002) (Figure 2c,d) and at a nonsignificant level in males ( $R^2 = 0.05258$ , *P*-value = 0.4976) (Figure 2e,f). However, the positive expression correlation of these genes was evident in both females (Figure 2g,h) and males (Figure 2i,j) of an additional bulk RNA-seq data from the developing whole brain of *D. melanogaster* (GSE199164), supporting the positive correlation between expression level of *deathstar* and *Eaat1* genes.

### Coexpression of *deathstar* and *Eaat1* genes in *Drosophila* brain

To test whether *deathstar* gene is co-expressed with *Eaat1* in single cells of *Drosophila* brain, the driver

lines expressing GAL4 and LexA proteins under the control of *deathstar* and *Eaat1* promoters have been used. For this purpose, the male flies expressing GAL4 under the control of *deathstar* promoter and expressing LexA under the control of *Eaat1* promoter were crossed to the virgin females transgenic for both *UAS-mCD8RFP* and *lexAop-mCD8GFP* constructs (Table 1), so that the expression pattern of RFP and GFP in progenies will depict the expression pattern of *deathstar* and *Eaat1* genes, respectively. Results illustrated that the fluorescent signals corresponding to the *deathstar* expression (RFP) were overlapped with the *Eaat1* signals (GFP) in a defined set of single cells in *Drosophila* midbrain (Figure 3a). For this experiment, *Eaat1* and *repo* genes were used for astrocytes (green signals) and all glia (blue signals), respectively (Figure 3b). Quantification of data from three independent experiments showed that 64% of *deathstar* fluorescence signal overlapped with *Eaat1* signals (Figure 3c), suggesting colocalized expression of these genes in *Drosophila* brain. These ALG cells (coexpressing *deathstar* and *Eaat1* genes) comprised an average of 45.7% of all astrocytes in the *Drosophila* brain (Figure 3c). Also, 46% of the *deathstar* signals were overlapped with *repo*-expressing cells (Figure 3d). This population of glia (coexpressing *deathstar* and *repo* genes) composed an average of 33.9% of all glia in the *Drosophila* brain (Figure 3d). Using another *deathstar*-GAL4 line in an additional fluorescence imaging experiment also showed coexpression of *deathstar* and *Eaat1* genes in a set of ALG cells in the *Drosophila* optic lobe (Supplemental file S4). These data altogether pinpoint a set of ALG single cells in the *Drosophila* brain, coexpressing the *deathstar* and *Eaat1* genes.

### Sex-biased developmental effects of *deathstar* gene in *D. melanogaster*

For functional analysis of *deathstar* gene, its expression was suppressed using a specific RNAi expressed in female and male flies in a cell type-specific manner. To this end, virgin females transgenic for *deathstar*-RNAi construct were crossed to a set of male GAL4 driver lines, enabling their progenies to express the *deathstar*-RNAi in different neural cell types of *D. melanogaster*. We took advantage to use recently developed subtype glial-GAL4 drivers which are



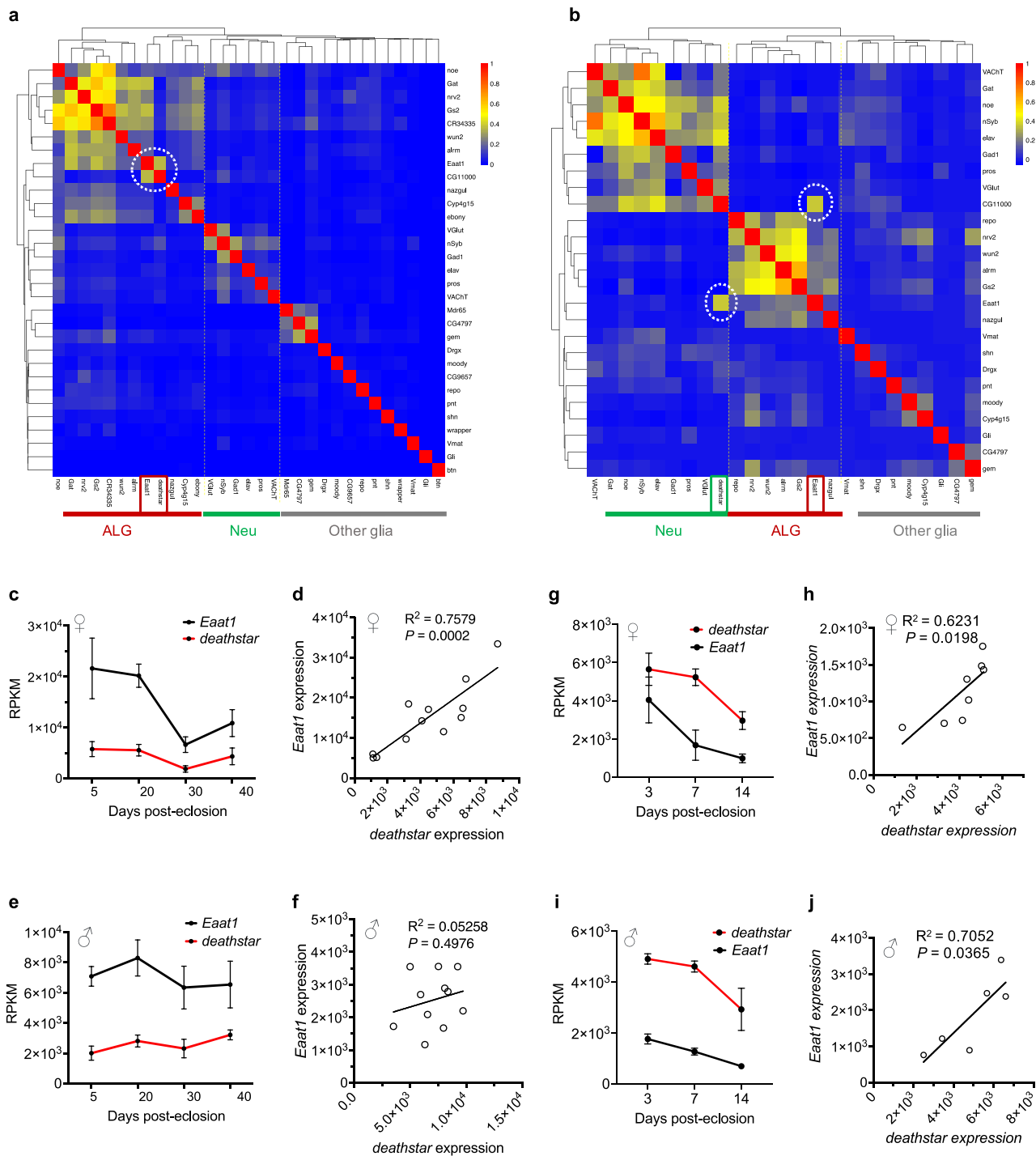


**Figure 2.** Positive expression correlation of *deathstar* with *Eaat1*. a) Heatmap analysis based on the Pearson correlation coefficient between *deathstar* and known molecular markers of *Drosophila* nervous system across sequenced single cells of *Drosophila* optic lobe ( $n = 120,000$  cells). *deathstar* is co-clustered with the ALG markers including *Eaat1* (dotted circle). b) Heatmap analysis based on the Pearson correlation coefficient between *deathstar* and known molecular markers of *Drosophila* nervous system across sequenced single cells of *Drosophila* mid-brain ( $n = 28,695$ ). Two dotted circles in the heatmap point to the positive expression correlation of *deathstar* with *Eaat1*, among other markers. c-d) Correlation analysis of *deathstar* and *Eaat1* expression level using a bulk RNA-seq data of developing whole brain from female *D. melanogaster* ( $n = 12$  flies). e-f) Correlation analysis of *deathstar* and *Eaat1* expression using a bulk RNA-seq data of developing whole brain of male *D. melanogaster* ( $n = 11$  flies). g-j) Significant expression correlation between *deathstar* and *Eaat1* genes across developmental time-points of female (g-h), and male (i-j) *D. melanogaster*, obtained from the bulk RNA-seq data analysis of developing whole brain of the flies.

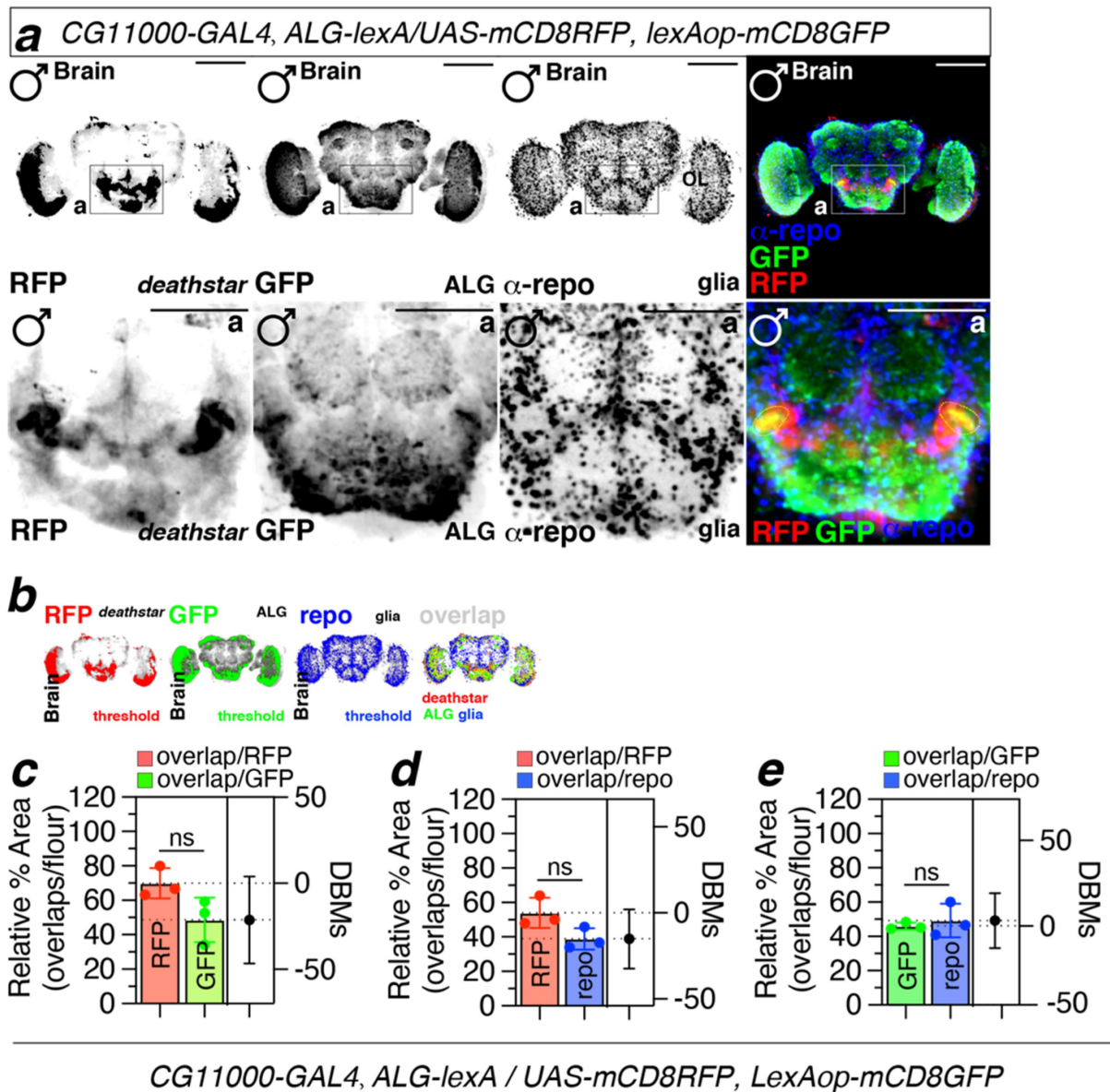


**Figure 3.** Coexpression of *deathstar* and *Eaat1* in the *Drosophila* brain. a) Overlapping fluorescence signals correspond to the *deathstar* (RFP, red) and *Eaat1* (GFP, green) expression, was shown in the midbrain of *D. melanogaster* (denoted as yellow dotted lines in the lower panel). Anti-repo antibody ( $\alpha$ -repo) was used for labeling the glia in the *Drosophila* brain (blue). Scale bars = 50  $\mu$ m. b) Results of the threshold function in ImageJ to differentiate real fluorescence signals from background for optimal quantification of overlapping fluorescent signals. Red signals denote *deathstar* (BDSC#: 91441), green signals denote *Eaat1* (BDSC#: 52719), and blue signals denote *repo* expression. c-e) Quantification data of the overlapping signals between *deathstar* and *Eaat1* (c), between *deathstar* and *Repo* (d), and between *Eaat1* and *Repo* genes (e).

feasibly expressed both in larval and adult subtype glial populations to determine which subtypes of glia is responsible for this phenotype [16,74]. The flies with the same genetic background but without *deathstar-RNAi* expression were used as the control group of this experiment (Table 2).

Through counting the eclosed flies of the crosses, unexpectedly, we observed a sex-biased eclosion rate for the progenies expressing *deathstar-RNAi*,

wherein most males expressing *deathstar-RNAi* did not develop into adult flies (Figure 4a), while the females with the same genotypes normally developed into adults (Figure 4b), suggesting a male-specific developmental function for *deathstar*.

A parallel experiment with the same procedure was carried out using an off-target RNAi, which targets the *Drosophila* gene *CG15765* (but not *deathstar*), and the results showed a standard ratio of males over females

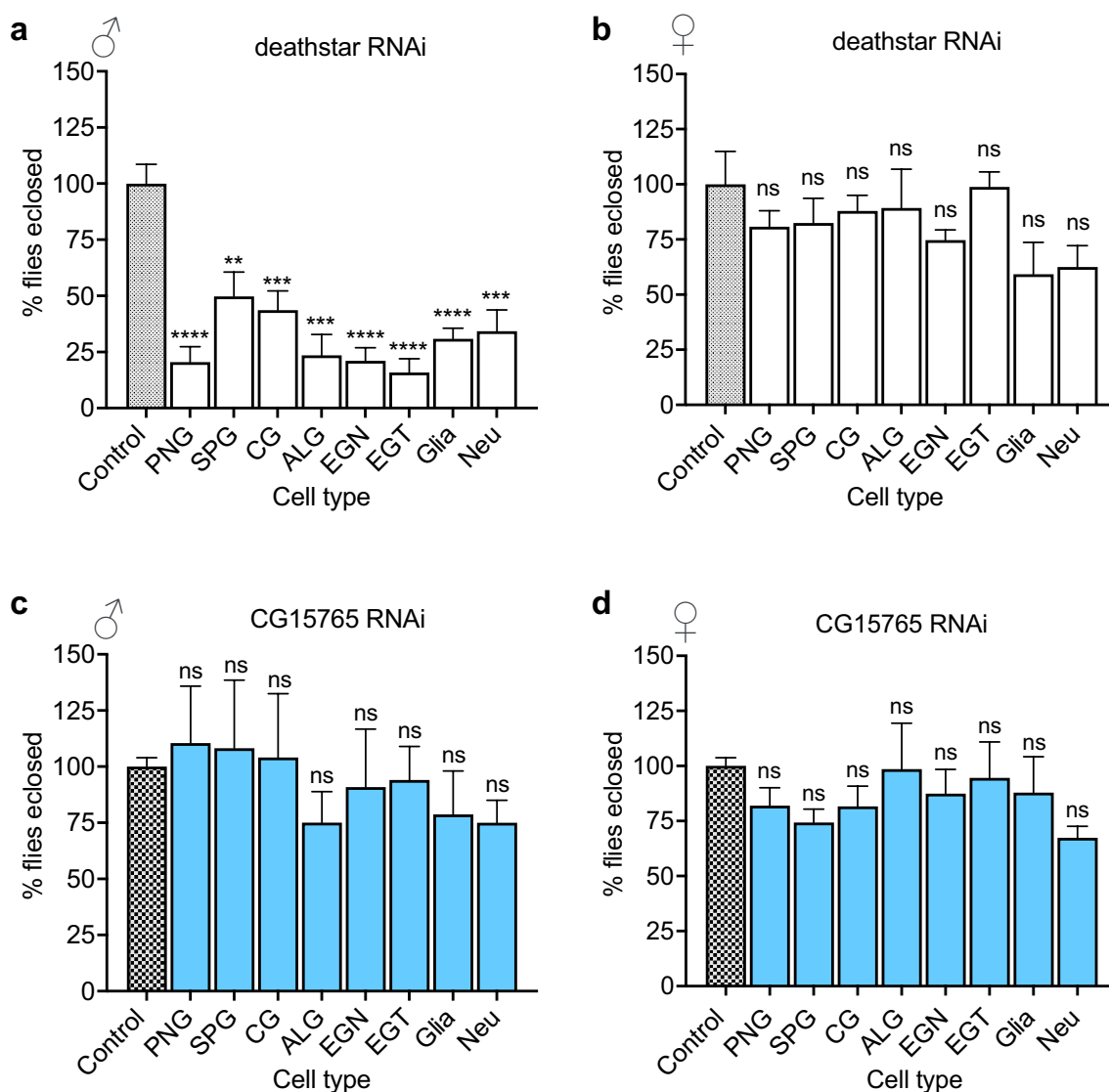


**Figure 4.** The effects of *deathstar* knock-down on normal development of *D. melanogaster*. a) In comparison with the control group, the majority of male progenies with *deathstar* knock-down did not develop into adults, indicated by significant reduction in eclosion rate (%). b) *Deathstar* knock-down in females did not show any developmental defects. Differences between the eclosion rates (%) of control group and the progenies with cell type-specific *deathstar* knock-down were not statistically significant (ns = nonsignificant). c-d) Eclosion rate of the progenies expressing an off-target RNAi, targeting the *Drosophila* CG15765 gene but not *deathstar*. The eclosion rate (%) was similar for all groups in both males and females.

(~1) for all progenies which expressed *CG15765-RNAi* (Figure 4c,d), supporting the specificity of *deathstar* RNAi to impede development of male progenies.

### **Deathstar affects locomotion and lifespan in *D. melanogaster***

As revealed by this study, the expression level of *deathstar* and *Eaat1* are positively correlated. On the other hand, *Eaat1* is a well-known astrocytic marker whose expression in astrocytes was shown to be critical to locomotion activities in

*D. melanogaster* [68]. To investigate if *deathstar* could also affect locomotion in *D. melanogaster*, locomotion assay was performed on adult flies which expressed *deathstar-RNAi* specifically in astrocytes. Results showed that the flies with the expression of *deathstar-RNAi* in their astrocytes had defects in their locomotion activity in comparison with the control group, shown by reduced forward velocity values per second in a 200-second time course (Figures 5a and 5c). Also, the average forward velocity rate of these flies revealed remarkable decreases in the locomotion activity

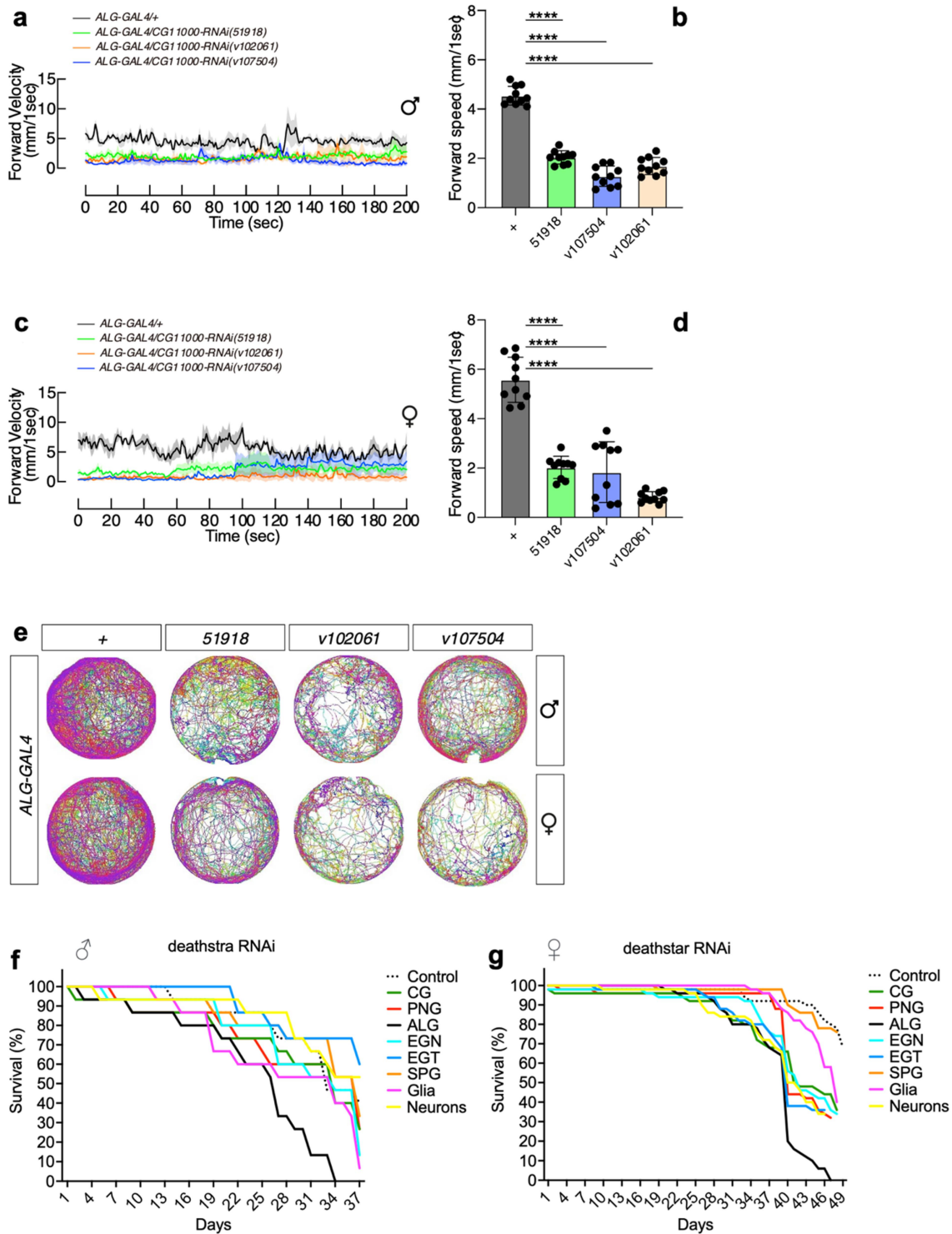


**Figure 5.** The effects of *deathstar* knock-down on the locomotion and lifespan of adult flies. a) Expression suppression of *deathstar* in astrocytes of male flies resulted in the decreased level of forward velocity per second, in a 200-second time course, in comparison with the control groups which do not express any RNAi (denoted as grey/black lines). b) Average velocity rate of the flies with suppressed *deathstar* expression in comparison with the control group ( $P$ -value  $< 0.0001$ ). c) Expression suppression of *deathstar* in astrocytes of female flies resulted in the decreased level of forward velocity per second, in a 200-second time course, in comparison with the control groups which lacked RNAi expression. d) Average velocity rate of the flies with suppressed *deathstar* expression in comparison with the control group ( $P$ -value  $< 0.0001$ ). e) Trajectory map analysis of the flies in the RNAi groups versus control groups, illustrating impeded locomotion activities in both male and female flies with suppressed expression level of *deathstar* using three different RNAi lines. f–g) ALG-specific reduction of lifespan in both male and female *D. melanogaster*, under expression suppression of *deathstar* gene.

of the flies expressing *deathstar* RNAi in their astrocytes (Figures 5b and 5d), suggesting the crucial role of *deathstar* in astrocytes.

Moreover, trajectory map analysis illustrated the reduced locomotion activity of the flies under suppression of *deathstar* expression in astrocytes, which was confirmed by using different independent RNAi lines (Figure 5e). The astrocyte-specific effects of *deathstar*-RNAi on locomotion behaviors of *D. melanogaster* were identified in both male (Figure 5a,b) and female (Figure 5c,d) flies, suggesting that the function of *deathstar* gene on *Drosophila* locomotion is not sexually dimorphic.

To test the possible function of *deathstar* gene in *D. melanogaster* lifespan, we suppressed its expression in different cell types through expressing the *deathstar* RNAi under regulation of cell type-specific GAL4 expression, then their lifespan for 40 ~ 50 days was measured. The most remarkable decreases in the lifespan were identified for the flies expressing the *deathstar*-RNAi specifically in their ALG cells (Figure 5f,g), supporting the astrocytic function of *deathstar* in shortening the lifespan of *D. melanogaster*. The ALG-specific effects of *deathstar*-RNAi on lifespan was also identified in both male (Figure 5f) and female (Figure 5g) flies, suggesting that the function of *deathstar* gene on *Drosophila* lifespan is not sexually dimorphic.

## Discussion

Like other metazoans, the *D. melanogaster* brain is formed by a large number of neurons and glia, each with distinct transcriptome profile conferring them unique structural and/or functional characteristics [63,75]. Cells do not act individually in brain but instead they make several clusters of single cells (known as cell types [10]) with specialized function and/or organization within neural circuits [76–78]. PNG, SPG, CG, EG and neurons are the main well-characterized cell types in the *Drosophila* nervous system [9,15,16,79,80].

Moreover, establishing and maintaining the identity of these cell types throughout the lifespan of the fly require expression of unique set of genes, known as molecular markers [9,15,16,23]. These markers are mostly the genes whose expression implements particular molecular pathways to specialize the development and/or function of the

respective cell types [81,82]. In this study, we used the previously known cell type-specific markers (Figure 1a) to classify the sequenced single cells of *Drosophila* optic lobe into their corresponding cell types. At least, two different molecular markers per each cell type were used for this purpose. These markers were among the best well-characterized ones in *D. melanogaster*, whose GAL4/UAS driver lines were also used frequently in previous studies for characterization, mapping and functional analysis of the respective cell types [9,15,16,25,79,80].

On the other hand, availability of the transcriptome profile of *Drosophila* brain at single-cell level enabled us to re-examine the identity of our classified cells, based on their similarities in their entire transcriptome. As the result, the single cells belonging to the ALG cell type (astrocytes) exhibited a far distinctive transcriptome profile versus PNG, SPG, CG, EG and neurons when they were classified based on the expression pattern of their markers (Figure 1b,c). Differential gene expression analysis showed significant enrichment of 11 genes while depletion of 6 genes in the identified ALG clusters (Figure 1e,f). In addition, while most of these identified ALG-enriched genes were among the previously reported ALG-enriched/specific markers, the *Eaat1* and *CR40469* genes were determined as neuronal markers by Konstantinides et al. [25]. These findings led us to focus on these genes which we found them as the top ALG-enriched genes (Supplemental file S1), and also myriad number of previous studies characterized the *Eaat1* as an astrocytic marker [10], and no cell type specificity was reported for *CR40469*, yet.

*CR40469* (also known as *lncRNA:CR40469*) spans a region of 213 kb on the X chromosome of *D. melanogaster* (NCBI GenBank, 2024 update). This gene is known to encode a long noncoding RNA (lncRNA) with 214 nucleotides with unknown function [83–85]. Moreover, due to the high sequence identity rate between *CR40469* gene and the glial marker *CG34335*, functional study of *CR40469* via RNAi-based strategies will be challenging. In a study by Rois et al. [86], a genomic knock-out of this gene in *D. melanogaster* was constructed and through differential gene expression analysis the greatest expression level

alterations were found for the genes located on the *Drosophila* chromosome X, nearby the *CR40469* locus (e.g. *CG42259*, *png*, and *CG4313* genes). According to this data, a trans-acting function was attributed to the *CR40469* lncRNA, by which it regulates the expression of its neighboring genes on chromosome X [86]. Here we found that the expression pattern of *CR40469* across the single cells of *Drosophila* optic lobe resembled that of *CR34335* gene which is consistent with previous studies which reported the *CR34335* gene as a glial marker [63]. Also, consistent with our results for ALG-enrichment of *CG40469* lncRNA, it was found by Croset et al. [26] as a glial and astrocyte-enriched gene, suggesting its pivotal role in these cell types. However, further functional studies are required to elucidate the mechanistic role of *CR40469* in its corresponding cell types.

Unlike *CR40469* gene, *Eaat1* is a well-characterized gene crucial for the development, physiology, and behaviors of *D. melanogaster*. When we categorized the sequenced single cells of *Drosophila* optic lobe based on their expression for *Eaat1*, we found the differential expression of an uncharacterized gene, named *CG11000* (we renamed it *deathstar*), which was significantly higher in *Eaat1*<sup>+</sup> cells versus the single cells without *Eaat1* expression (Figure 1i). This preliminary data compelled us to investigate the expression correlation of *Eaat1* and *deathstar* genes in *Drosophila* brain. Interestingly, the positive correlation was existed between these genes across the total set of single cells in *Drosophila* optic lobe and mid-brain, as well as across all developmental stages of *Drosophila* whole brain (Figure 2). Beside positive correlation, *deathstar* was clustered in the ALG cells of *Drosophila* optic lobe (Figure 2a), while clustered in the neuronal cluster in the mid-brain (Figure 2b) suggesting some non-ALG expression for this gene. In support of the positive expression correlation of *deathstar* and *Eaat1* genes, their expression level in the single-cell collection of *Drosophila* adult brain was analyzed in SCoPe database [87], and a significant positive correlation was observed ( $R^2 = 0.661$ ,  $P < 0.0001$ ; supplemental file S3).

Our data also provide a comparative assessment between two approaches of cell type identification: 1-cell type identification based on the predefined

set of molecular markers, and 2- cell type identification based on the similarities in whole transcriptome profile.

Since a set of multiple marker genes could not represent the complete genetic profile of a respective cell type, and on the other hand, different cell types may have similar transcriptome profile but differ only in the expression pattern of a limited number of genes, each of the above-mentioned approaches has its own pros and cons that should be considered for cell type identification purposes. For instance, *Eaat1* expression pattern *per se* could not distinguish ALG cells from other cell types since *Eaat1* was shown to be expressed also in a subset of neurons [25]. Similarly, some clusters in the Konstantinides et al. study were identified as neurons based on their entire transcriptome profile (clusters # 4 and 14), while they were positive for the glial marker *repo* [25], which necessitate testing additional markers on these clusters to reveal their actual identity. Also, studies have shown that while Repo protein is a good marker for glial cells [88,89], its transcripts are lowly expressed and often not detected in glial clusters [90], which challenges the use of *repo* gene as a glial marker in RNA-seq data analyses.

In *Drosophila* research, the binary systems such as GAL4/UAS and LexA/LexAop are powerful genetic tools to map the expression pattern of a gene-of-interest against different cell types [14]. Here, we used these systems to trace the distribution of mCD8RFP and mCD8GFP signals across the *Drosophila* optic lobe driven by *deathstar* and *Eaat1* promoters, respectively. The overlapped fluorescent signals of these genes illustrated their co-expression in a set of single cells in *Drosophila* midbrain and optic lobe (Figure 3 and supplemental file S4). However, some single cells in the *Drosophila* brain did not show such co-expression pattern which is consistent with the observed expression pattern of the *deathstar* and *Eaat1* genes in a cluster of single cells in adult *Drosophila* brain obtained from SCoPe, wherein some single cells express *deathstar* transcripts while negative for *Eaat1* expression (Supplemental file S3).

Functional analysis of *deathstar* revealed a male-specific developmental function of this gene which was not cell type-specific (Figure 4a). Such sex-

biased developmental effect of the gene could suggest that *deathstar* may exert its functional role in the development of *D. melanogaster* through cellular and/or molecular pathways, which act differently in males and females. Further functional studies are required to elucidate the molecular mechanisms underlying the sex-biased effects of *deathstar* knock-down.

However, *deathstar* knock-down in adult flies resulted in a reduced locomotion activity in both sexes (males and females), suggesting that the effect of *deathstar* gene on locomotion behaviours of the fly is not sexually dimorphic (Figure 5a–e).

Besides changing the locomotion activities, *deathstar* knock-down resulted in shortened lifespan of both males and females in an ALG-specific manner (Figure 5f,g). This result highlights the crucial role of *deathstar* gene in normal lifespan of *D. melanogaster*, which is not sexually dimorphic.

Taken together, this study for the first time delineated the expression pattern and crucial role of the *deathstar* gene in normal development, locomotion and lifespan of *D. melanogaster*, which is an initial step toward further functional characterization of this gene.

## Acknowledgments

The stocks used in this study were from the Bloomington Drosophila Stock Center (NIH P40OD018537). We thank Khoi-Nguyen Ha Nguyen for his assistance in the experiments performed in this study. Special thanks to Hongyu Miao and Yanan Wei for their invaluable assistance. Their insights and support have greatly enriched its content.

## Disclosure statement

No potential conflict of interest was reported by the author(s).

## Data availability statement

The authors confirm that the data supporting the findings of this study are available within the article and its supplementary materials.

## ORCID

Hadi Najafi  <http://orcid.org/0000-0002-1885-6689>

Woo Jae Kim  <http://orcid.org/0000-0002-2826-4177>

## References

- [1] Tolwinski NS. Introduction: Drosophila—A model system for developmental biology. MDPI; 2017. p. 9.
- [2] Spindler SR, Hartenstein V. The Drosophila neural lineages: a model system to study brain development and circuitry. Dev Genes Evol. 2010;220(1–2):1–10. doi: 10.1007/s00427-010-0323-7
- [3] Zhu B, Pennack JA, McQuilton P, et al. Drosophila neurotrophins reveal a common mechanism for nervous system formation. PLoS Biol. 2008;6(11):e284. doi: 10.1371/journal.pbio.0060284
- [4] Neckameyer WS, Argue KJ. Comparative approaches to the study of physiology: Drosophila as a physiological tool. Am J Physiol Regul Integr Comp Physiol. 2013;304(3):R177–R88. doi: 10.1152/ajpregu.00084.2012
- [5] Shin M, Copeland JM, Venton BJ. Drosophila as a model system for neurotransmitter measurements. ACS Chem Neurosci. 2018;9(8):1872–1883. doi: 10.1021/acschemneuro.7b00456
- [6] Kim T, Song B, Lee I-S. Drosophila glia: models for human neurodevelopmental and neurodegenerative disorders. Int J Mol Sci. 2020;21(14):4859. doi: 10.3390/ijms21144859
- [7] Devineni AV, Scaplen KM. Neural circuits underlying behavioral flexibility: insights from Drosophila. Front Behav Neurosci. 2022;15:821680. doi: 10.3389/fnbeh.2021.821680
- [8] Huser A, Rohwedder A, Apostolopoulou AA, et al. The serotonergic central nervous system of the Drosophila larva: anatomy and behavioral function. PLOS ONE. 2012;7(10):e47518. doi: 10.1371/journal.pone.0047518
- [9] Yildirim K, Petri J, Kottmeier R, et al. Drosophila glia: Few cell types and many conserved functions. Glia. 2019;67(1):5–26. doi: 10.1002/glia.23459
- [10] Bittern J, Pogodalla N, Ohm H, et al. Neuron–glia interaction in the Drosophila nervous system. Dev Neurobiol. 2021;81(5):438–452. doi: 10.1002/dneu.22737
- [11] Mayer F, Mayer N, Chinn L, et al. Evolutionary conservation of vertebrate blood–brain barrier chemoprotective mechanisms in Drosophila. J Neurosci. 2009;29(11):3538–3550. doi: 10.1523/JNEUROSCI.5564-08.2009
- [12] DeSalvo MK, Hindle SJ, Rusan ZM, et al. The Drosophila surface glia transcriptome: evolutionary conserved blood–brain barrier processes. Front Neurosci. 2014;8:113393. doi: 10.3389/fnins.2014.00346
- [13] Pfeiffer BD, Jenett A, Hammonds AS, et al. Tools for neuroanatomy and neurogenetics in Drosophila. Proc Natl Acad Sci USA. 2008;105(28):9715–9720. doi: 10.1073/pnas.0803697105
- [14] Luan H, Diao F, Scott RL, et al. The Drosophila split Gal4 system for neural circuit mapping. Front Neural Circuits. 2020;14:603397. doi: 10.3389/fncir.2020.603397
- [15] Freeman MR. Drosophila central nervous system glia. Cold Spring harbor perspectives in biology. Cold

- Spring Harbor Perspect Biol. 2015;7(11):a020552. doi: [10.1101/cshperspect.a020552](https://doi.org/10.1101/cshperspect.a020552)
- [16] Kremer MC, Jung C, Batelli S, et al. The glia of the adult *Drosophila* nervous system. *Glia*. 2017;65(4):606–638. doi: [10.1002/glia.23115](https://doi.org/10.1002/glia.23115)
- [17] Jenett A, Rubin GM, Ngo T-T, et al. A GAL4-driver line resource for *Drosophila* neurobiology. *Cell Rep*. 2012;2(4):991–1001. doi: [10.1016/j.celrep.2012.09.011](https://doi.org/10.1016/j.celrep.2012.09.011)
- [18] Weaver LN, Ma T, Drummond-Barbosa D. Analysis of Gal4 expression patterns in adult *Drosophila* females. *G3: Genes Genomes Genetics*. 2020;10(11):4147–4158. doi: [10.1534/g3.120.401676](https://doi.org/10.1534/g3.120.401676)
- [19] Chen Y-C, Chen Y-C, Rajesh R, et al. Using single-cell RNA sequencing to generate predictive cell-type-specific split-GAL4 reagents throughout development. *Proc Natl Acad Sci USA*. 2023;120(32):e2307451120. doi: [10.1073/pnas.2307451120](https://doi.org/10.1073/pnas.2307451120)
- [20] Yeung K, Bollepogu Raja KK, Shim Y-K, et al. Single cell RNA sequencing of the adult *Drosophila* eye reveals distinct clusters and novel marker genes for all major cell types. *Commun Biol*. 2022;5(1):1370. doi: [10.1038/s42003-022-04337-1](https://doi.org/10.1038/s42003-022-04337-1)
- [21] Bollepogu Raja KK, Yeung K, Shim Y-K, et al. A single cell genomics atlas of the *Drosophila* larval eye reveals distinct photoreceptor developmental timelines. *Nat Commun*. 2023;14(1):7205. doi: [10.1038/s41467-023-43037-0](https://doi.org/10.1038/s41467-023-43037-0)
- [22] Fu Y, Huang X, Zhang P, et al. Single-cell RNA sequencing identifies novel cell types in *Drosophila* blood. *J Genet Genome*. 2020;47(4):175–186. doi: [10.1016/j.jgg.2020.02.004](https://doi.org/10.1016/j.jgg.2020.02.004)
- [23] Henry GL, Davis FP, Picard S, et al. Cell type-specific genomics of *Drosophila* neurons. *Nucleic Acids Res*. 2012;40(19):9691–9704. doi: [10.1093/nar/gks671](https://doi.org/10.1093/nar/gks671)
- [24] Palmateer CM, Artikis C, Brovero SG, et al. Single-cell transcriptome profiles of *Drosophila* fruitless-expressing neurons from both sexes. *Elife*. 2023;12:e78511. doi: [10.7554/eLife.78511](https://doi.org/10.7554/eLife.78511)
- [25] Konstantinides N, Kapuralin K, Fadil C, et al. Phenotypic convergence: distinct transcription factors regulate common terminal features. *Cell*. 2018;174(3):622–35. e13. doi: [10.1016/j.cell.2018.05.021](https://doi.org/10.1016/j.cell.2018.05.021)
- [26] Croset V, Treiber CD, Waddell S. Cellular diversity in the *Drosophila* midbrain revealed by single-cell transcriptomics. *Elife*. 2018;7:e34550. doi: [10.7554/eLife.34550](https://doi.org/10.7554/eLife.34550)
- [27] Pacifico R, MacMullen CM, Walkinshaw E, et al. Brain transcriptome changes in the aging *Drosophila melanogaster* accompany olfactory memory performance deficits. *PLOS ONE*. 2018;13(12):e0209405. doi: [10.1371/journal.pone.0209405](https://doi.org/10.1371/journal.pone.0209405)
- [28] Babicki S, Arndt D, Marcu A, et al. Heatmapper: web-enabled heat mapping for all. *Nucleic Acids Res*. 2016;44(W1):W147–W53. doi: [10.1093/nar/gkw419](https://doi.org/10.1093/nar/gkw419)
- [29] Wickham H. *ggplot2: Elegant Graphics for Data Analysis*. Use R!. Springer International Publishing, Cham; 2016. p. 203–220. doi: [10.1007/978-3-319-24277-4\\_10](https://doi.org/10.1007/978-3-319-24277-4_10)
- [30] Kolde R, Kolde MR. Package ‘pheatmap’. *R Package*. 2015;1(7):790.
- [31] Ritchie ME, Phipson B, Wu D, et al. *limma* powers differential expression analyses for RNA-sequencing and microarray studies. *Nucleic Acids Res*. 2015;43(7):e47–e. doi: [10.1093/nar/gkv007](https://doi.org/10.1093/nar/gkv007)
- [32] Schober P, Vetter TR. Two-sample unpaired t tests in medical research. *Anesthesia Analgesia*. 2019;129(4):911. doi: [10.1213/ANE.0000000000004373](https://doi.org/10.1213/ANE.0000000000004373)
- [33] Oliveros JV. An interactive tool for comparing lists with Venn’s diagrams. 2007–2015. 2016 [cited 2021 Jul 15].
- [34] Sievers F, Wilm A, Dineen D, et al. Fast, scalable generation of high-quality protein multiple sequence alignments using clustal omega. *Mol Syst Biol*. 2011;7(1):539. doi: [10.1038/msb.2011.75](https://doi.org/10.1038/msb.2011.75)
- [35] Goujon M, McWilliam H, Li W, et al. A new bioinformatics analysis tools framework at EMBL–EBI. *Nucleic Acids Res*. 2010;38(suppl\_2):W695–W699. doi: [10.1093/nar/gkq313](https://doi.org/10.1093/nar/gkq313)
- [36] Guo A, Li L, Xia S, et al. Conditioned visual flight orientation in *Drosophila*: dependence on age, practice, and diet. *Learn Memory*. 1996;3(1):49–59. doi: [10.1101/lm.3.1.49](https://doi.org/10.1101/lm.3.1.49)
- [37] Brand AH, Perrimon N. Targeted gene expression as a means of altering cell fates and generating dominant phenotypes. *Development*. 1993;118(2):401–415. doi: [10.1242/dev.118.2.401](https://doi.org/10.1242/dev.118.2.401)
- [38] Hawley HR, Roberts CJ, Fitzsimons HL. Comparison of neuronal GAL4 drivers along with the AGES (auxin-inducible gene expression system) and TARGET (temporal and regional gene expression targeting) systems for fine tuning of neuronal gene expression in *Drosophila*. *MicroPubl Biol*. 2023;2023. doi: [10.17912/micropub.biology.000885](https://doi.org/10.17912/micropub.biology.000885)
- [39] Kim WJ, Jan LY, Jan YN. A PDF/NPF neuropeptide signaling circuitry of male *Drosophila melanogaster* controls rival-induced prolonged mating. *Neuron*. 2013;80(5):1190–1205. doi: [10.1016/j.neuron.2013.09.034](https://doi.org/10.1016/j.neuron.2013.09.034)
- [40] Wu JS, Luo L. A protocol for dissecting *Drosophila melanogaster* brains for live imaging or immunostaining. *Nat Protoc*. 2006;1(4):2110–2115. doi: [10.1038/nprot.2006.336](https://doi.org/10.1038/nprot.2006.336)
- [41] Schneider CA, Rasband WS, Eliceiri KW. NIH Image to ImageJ: 25 years of image analysis. *Nat Methods*. 2012;9(7):671. doi: [10.1038/nmeth.2089](https://doi.org/10.1038/nmeth.2089)
- [42] Mi K, Li Y, Yang Y, et al. DVT: a high-throughput analysis pipeline for locomotion and social behavior in adult *Drosophila melanogaster*. *Cell Biosci*. 2023;13(1):187. doi: [10.1186/s13578-023-01125-0](https://doi.org/10.1186/s13578-023-01125-0)
- [43] Scaplen KM, Mei NJ, Bounds HA, et al. Automated real-time quantification of group locomotor activity in *Drosophila melanogaster*. *Sci Rep*. 2019;9(1):4427. doi: [10.1038/s41598-019-40952-5](https://doi.org/10.1038/s41598-019-40952-5)



- [44] Linford NJ, Bilgir C, Ro J, et al. Measurement of Lifespan in *Drosophila melanogaster*. *J Vis Exp*. 2013 71;(71):e50068. doi: [10.3791/50068-v](https://doi.org/10.3791/50068-v)
- [45] Stalpers LJ, Kaplan EL, Edward L. Kaplan and the Kaplan-Meier survival curve. *BSHM Bull: J Br Soc For the Hist Off Math*. 2018;33(2):109–135. doi: [10.1080/17498430.2018.1450055](https://doi.org/10.1080/17498430.2018.1450055)
- [46] Brunet Avalos C, Maier GL, Bruggmann R, et al. Single cell transcriptome atlas of the *Drosophila* larval brain. *Elife*. 2019;8:e50354. doi: [10.7554/eLife.50354](https://doi.org/10.7554/eLife.50354)
- [47] McLaughlin CN, Brbić M, Xie Q, et al. Single-cell transcriptomes of developing and adult olfactory receptor neurons in *Drosophila*. *Elife*. 2021;10:e63856. doi: [10.7554/eLife.63856](https://doi.org/10.7554/eLife.63856)
- [48] Deitcher DL, Ueda A, Stewart BA, et al. Distinct requirements for evoked and spontaneous release of neurotransmitter are revealed by mutations in the *Drosophila* gene neuronal-synaptobrevin. *J Neurosci*. 1998;18(6):2028–2039. doi: [10.1523/JNEUROSCI.18-06-02028.1998](https://doi.org/10.1523/JNEUROSCI.18-06-02028.1998)
- [49] Robinow S, White K. Characterization and spatial distribution of the ELAV protein during *drosophila melanogaster* development. *J Neurobiol*. 1991;22(5):443–461. doi: [10.1002/neu.480220503](https://doi.org/10.1002/neu.480220503)
- [50] Peco E, Davla S, Camp DM, et al. *Drosophila* astrocytes cover specific territories of the CNS neuropil and are instructed to differentiate by Prospero, a key effector of Notch. *Development*. 2016;143(7):1170–1181. doi: [10.1242/dev.133165](https://doi.org/10.1242/dev.133165)
- [51] Huang Y, Ng FS, Jackson FR. Comparison of larval and adult *drosophila* astrocytes reveals stage-specific gene expression profiles. *G3. Genes Genomes Genetics*. 2015;5(4):551–558. doi: [10.1534/g3.114.016162](https://doi.org/10.1534/g3.114.016162)
- [52] Doherty J, Logan MA, Taşdemir ÖE, et al. Ensheathing glia function as phagocytes in the adult *Drosophila* brain. *J Neurosci*. 2009;29(15):4768–4781. doi: [10.1523/JNEUROSCI.5951-08.2009](https://doi.org/10.1523/JNEUROSCI.5951-08.2009)
- [53] Sinakevitch I, Grau Y, Strausfeld NJ, et al. Dynamics of glutamatergic signaling in the mushroom body of young adult *Drosophila*. *Neural Dev*. 2010;5(1):10–20. doi: [10.1186/1749-8104-5-10](https://doi.org/10.1186/1749-8104-5-10)
- [54] Suh J, Jackson FR. *Drosophila* ebony activity is required in glia for the circadian regulation of locomotor activity. *Neuron*. 2007;55(3):435–447. doi: [10.1016/j.neuron.2007.06.038](https://doi.org/10.1016/j.neuron.2007.06.038)
- [55] Stork T, Sheehan A, Tasdemir-Yilmaz OE, et al. Neuron-glia interactions through the Heartless FGF receptor signaling pathway mediate morphogenesis of *Drosophila* astrocytes. *Neuron*. 2014;83(2):388–403. doi: [10.1016/j.neuron.2014.06.026](https://doi.org/10.1016/j.neuron.2014.06.026)
- [56] Dillon N, Cocanougher B, Sood C, et al. Single cell RNA-seq analysis reveals temporally-regulated and quiescence-regulated gene expression in *Drosophila* larval neuroblasts. *Neural Dev*. 2022;17(1):1–18. doi: [10.1186/s13064-022-00163-7](https://doi.org/10.1186/s13064-022-00163-7)
- [57] Schwabe T, Bainton RJ, Fetter RD, et al. GPCR signaling is required for blood-brain barrier formation in *Drosophila*. *Cell*. 2005;123(1):133–144. doi: [10.1016/j.cell.2005.08.037](https://doi.org/10.1016/j.cell.2005.08.037)
- [58] Bainton RJ, Tsai L-Y, Schwabe T, et al. moody encodes two GPCRs that regulate cocaine behaviors and blood-brain barrier permeability in *Drosophila*. *Cell*. 2005;123(1):145–156. doi: [10.1016/j.cell.2005.07.029](https://doi.org/10.1016/j.cell.2005.07.029)
- [59] Rujano MA, Briand D, Đelić B, et al. An interplay between cellular growth and atypical fusion defines morphogenesis of a modular glial niche in *Drosophila*. *Nat Commun*. 2022;13(1):4999. doi: [10.1038/s41467-022-32685-3](https://doi.org/10.1038/s41467-022-32685-3)
- [60] Speder P, Brand AH. Systemic and local cues drive neural stem cell niche remodelling during neurogenesis in *Drosophila*. *Elife*. 2018;7:e30413. doi: [10.7554/eLife.30413](https://doi.org/10.7554/eLife.30413)
- [61] Sheng L, Shields EJ, Gospocic J, et al. Social reprogramming in ants induces longevity-associated glia remodeling. *Sci Adv*. 2020;6(34):eaba9869. doi: [10.1126/sciadv.aba9869](https://doi.org/10.1126/sciadv.aba9869)
- [62] Ren Q, Awasaki T, Wang Y-C, et al. Lineage-guided Notch-dependent gliogenesis by *Drosophila* multi-potent progenitors. *Development*. 2018;145(11):dev160127. doi: [10.1242/dev.160127](https://doi.org/10.1242/dev.160127)
- [63] Davie K, Janssens J, Koldere D, et al. A single-cell transcriptome atlas of the aging *Drosophila* brain. *Cell*. 2018;174(4):982–98. e20. doi: [10.1016/j.cell.2018.05.057](https://doi.org/10.1016/j.cell.2018.05.057)
- [64] Holcroft CE, Jackson WD, Lin W-H, et al. Innexin ogle and *Inx2* are required in glial cells for normal postembryonic development of the *drosophila* central nervous system. *J Cell Sci*. 2013;126(17):3823–3834. doi: [10.1242/jcs.117994](https://doi.org/10.1242/jcs.117994)
- [65] Luna AJF, Perier M, Seugnet L. Amyloid precursor protein in *drosophila* glia regulates sleep and genes involved in glutamate recycling. *J Neurosci*. 2017;37(16):4289–4300. doi: [10.1523/JNEUROSCI.2826-16.2017](https://doi.org/10.1523/JNEUROSCI.2826-16.2017)
- [66] Chaturvedi R, Reddig K, H-S L. Long-distance mechanism of neurotransmitter recycling mediated by glial network facilitates visual function in *Drosophila*. *Proc Natl Acad Sci USA*. 2014;111(7):2812–2817. doi: [10.1073/pnas.1323714111](https://doi.org/10.1073/pnas.1323714111)
- [67] Hartenstein V. Morphological diversity and development of glia in *Drosophila*. *Glia*. 2011;59(9):1237–1252. doi: [10.1002/glia.21162](https://doi.org/10.1002/glia.21162)
- [68] Stacey SM, Muraro NI, Peco E, et al. *Drosophila* glial glutamate transporter *Eaat1* is regulated by fringe-mediated notch signaling and is essential for larval locomotion. *J Neurosci*. 2010;30(43):14446–14457. doi: [10.1523/JNEUROSCI.1021-10.2010](https://doi.org/10.1523/JNEUROSCI.1021-10.2010)
- [69] You S, Yu AM, Roberts MA, et al. Circadian regulation of the *Drosophila* astrocyte transcriptome. *PLoS Genet*. 2021;17(9):e1009790. doi: [10.1371/journal.pgen.1009790](https://doi.org/10.1371/journal.pgen.1009790)
- [70] Corrales M, Cocanougher BT, Kohn AB, et al. A single-cell transcriptomic atlas of complete insect nervous systems across multiple life stages. *Neural Dev*. 2022;17(1):8. doi: [10.1186/s13064-022-00164-6](https://doi.org/10.1186/s13064-022-00164-6)
- [71] Rival T, Soustelle L, Cattaert D, et al. Physiological requirement for the glutamate transporter dEAT1 at

- the adult drosophila neuromuscular junction. *J Neurobiol.* 2006;66(10):1061–1074. doi: [10.1002/neu.20270](https://doi.org/10.1002/neu.20270)
- [72] Freeman MR, Delrow J, Kim J, et al. Unwrapping glial biology: Gcm target genes regulating glial development, diversification, and function. *Neuron.* 2003;38(4):567–580. doi: [10.1016/S0896-6273\(03\)00289-7](https://doi.org/10.1016/S0896-6273(03)00289-7)
- [73] Gramates LS, Agapite J, Attrill H, et al. FlyBase: a guided tour of highlighted features. *Genetics.* 2022;220(4):iyac035. doi: [10.1093/genetics/iyac035](https://doi.org/10.1093/genetics/iyac035)
- [74] Miao H, Wei Y, Lee SG, et al. Glia-specific expression of neuropeptide receptor Lgr4 regulates development and adult physiology in Drosophila. *J of Neurosci Res.* 2024;102(1):e25271. doi: [10.1002/jnr.25271](https://doi.org/10.1002/jnr.25271)
- [75] Urbach R, Technau GM. Molecular markers for identified neuroblasts in the developing brain of Drosophila. *Development.* 2003;130(16):3621–3637. doi: [10.1242/dev.00533](https://doi.org/10.1242/dev.00533)
- [76] Schneider-Mizell CM, Gerhard S, Longair M, et al. Quantitative neuroanatomy for connectomics in Drosophila. *Elife.* 2016;5:e12059. doi: [10.7554/eLife.12059](https://doi.org/10.7554/eLife.12059)
- [77] Sterne GR, Otsuna H, Dickson BJ, et al. Classification and genetic targeting of cell types in the primary taste and premotor center of the adult Drosophila brain. *Elife.* 2021;10:e71679. doi: [10.7554/eLife.71679](https://doi.org/10.7554/eLife.71679)
- [78] Malin J, Desplan C. Neural specification, targeting, and circuit formation during visual system assembly. *Proc Natl Acad Sci USA.* 2021;118(28):e2101823118. doi: [10.1073/pnas.2101823118](https://doi.org/10.1073/pnas.2101823118)
- [79] Awasaki T, Lai S-L, Ito K, et al. Organization and postembryonic development of glial cells in the adult central brain of Drosophila. *J Neurosci.* 2008;28(51):13742–13753. doi: [10.1523/JNEUROSCI.4844-08.2008](https://doi.org/10.1523/JNEUROSCI.4844-08.2008)
- [80] Stork T, Bernardos R, Freeman MR. Analysis of glial cell development and function in Drosophila. *Cold Spring Harb Protoc.* 2012;(1):1. doi: [10.1101/pdb.top067587](https://doi.org/10.1101/pdb.top067587)
- [81] Crews ST. Drosophila embryonic CNS development: neurogenesis, gliogenesis, cell fate, and differentiation. *Genetics.* 2019;213(4):1111–1144. doi: [10.1534/genetics.119.300974](https://doi.org/10.1534/genetics.119.300974)
- [82] Jones BW. Glial cell development in the drosophila embryo. *BioEssays.* 2001;23(10):877–887. doi: [10.1002/bies.1129](https://doi.org/10.1002/bies.1129)
- [83] Ueda M, Sato T, Ohkawa Y, et al. Identification of miR-305, a micro RNA that promotes aging, and its target mRNA s in Drosophila. *Genes Cells.* 2018;23(2):80–93. doi: [10.1111/gtc.12555](https://doi.org/10.1111/gtc.12555)
- [84] Zhang L, Zhang S, Wang R, et al. Genome-wide identification of long noncoding RNA and their potential interactors in ISWI mutants. *Int J Mol Sci.* 2022;23(11):6247. doi: [10.3390/ijms23116247](https://doi.org/10.3390/ijms23116247)
- [85] Baker BM, Mokashi SS, Shankar V, et al. The Drosophila brain on cocaine at single-cell resolution. *Genome Res.* 2021;31(10):1927–1937. doi: [10.1101/gr.268037.120](https://doi.org/10.1101/gr.268037.120)
- [86] Amador Rios R. Unravelling the role of long noncoding RNAs in the context of cell-growth and regeneration [Doctoral dissertation]. Universitat de Barcelona; 2022.
- [87] Li H, Janssens J, De Waegeneer M, et al. Fly cell atlas: a single-nucleus transcriptomic atlas of the adult fruit fly. *Science.* 2022;375(6584):eabk2432. doi: [10.1126/science.abk2432](https://doi.org/10.1126/science.abk2432)
- [88] Xiong W-C, Okano H, Patel NH, et al. repo encodes a glial-specific homeo domain protein required in the drosophila nervous system. *Genes Dev.* 1994;8(8):981. doi: [10.1101/gad.8.8.981](https://doi.org/10.1101/gad.8.8.981)
- [89] Yuasa Y, Okabe M, Yoshikawa S, et al. Drosophila homeodomain protein REPO controls glial differentiation by cooperating with ETS and BTB transcription factors. *Development.* 2003;130(11):2419–2428. doi: [10.1242/dev.00468](https://doi.org/10.1242/dev.00468)
- [90] Ferreira AGA, Desplan C. An atlas of the developing drosophila visual system glia and subcellular mRNA localization of transcripts in single cells. *bioRxiv.* 2023:2023.08.06.552169.